Front. Earth Sci. 2011, 5(1): 23–36
DOI 10.1007/s11707-011-0162-5

RESEARCH ARTICLE

Geomicrobiological perspective on the pattern and causes of the 5-million-year Permo/Triassic biotic crisis

Shucheng XIE (✉)[1], Yongbiao WANG[2]

1 Key Laboratory of Biogeology and Environmental Geology (Ministry of Education), China University of Geosciences, Wuhan 430074, China
2 State Key Laboratory of Geological Processes and Mineral Resources, China University of Geosciences, Wuhan 430074, China

Abstract The pattern and causes of Permo/Triassic biotic crisis were mainly documented by faunal and terrestrial plant records. We reviewed herein the geomicrobiological perspective on this issue based on the reported cyanobacterial record. Two episodic cyanobacterial blooms were observed to couple with carbon isotope excursions and faunal mass extinction at Meishan section, suggestive of the presence of at least two episodic biotic crises across the Permian-Triassic boundary (PTB). The two episodes of cyanobacterial blooms, carbon isotope excursions and faunal mass extinction were, respectively, identified in several sections of the world, inferring the presence of two global changes across the PTB. Close associations among the three records (cyanobacterial bloom, shift in carbon isotope composition, and faunal extinction) were subsequently observed in three intervals in the Early Triassic, the protracted recovery period as previously thought, inferring the occurrence of more episodes of global changes. Spatiotemporal association of cyanobacterial blooms with volcanic materials in South China, and probably in South-east Asia, infers their causal relationship. Volcanism is believed to trigger the biotic crisis in several ways and to cause the close association among microbial blooms, the carbon isotope excursions and faunal mass extinctions in four intervals from the latest Permian to the Early Triassic. The major episodes of the well-known Siberian flood eruption are proposed to be responsible for the extinctions in the Early Triassic, but their synchronicity with the end-Permian extinction awaits more precise dating data to confirm. Geomicrobial records are thus suggestive of a long-term episodic biotic crisis (at least four episodes) lasting from the latest Permian to the end of the Early Triassic, induced by the global volcanic eruptions and sea level changes during Pangea formation.

Received March 12, 2010; accepted June 18, 2010

E-mail: xiecug@163.com

Keywords geobiology, microbial bloom, molecular fossils, microbialite, Siberian basalt, volcanism, sea level change

1 Introduction

Permo/Triassic biotic crisis is believed to be the most severe and protracted one in Phanerozoic. The pattern and causes of the mortality are still in debate, with the paleontology records being mainly from faunas and higher plants. Recently, the microbial records, such as cyanobacteria and green sulfur bacteria, are paid great attention to and are used to infer the pattern (Xie et al., 2005; 2007), as well as the potential triggers (Grice et al., 2005, Xie et al., 2010) of the faunal extinction across the Permian-Triassic boundary (PTB). Microbes, being the base member in the food chain, are the important components within an ecosystem, which not only interact with the surrounding environments but also show strong connection with the faunas. Any changes in both the environmental conditions and the faunas of various trophic levels could be recorded by the microbial fingerprints. At this point, the pattern and causes of the faunal mass extinction across the PTB could be, partly if not wholly, reflected by the microbial records, particularly by the functional groups of microbes.

However, survey on microbes is a tough work in sedimentary rocks, arising from two critical issues. First, the microbes are usually hard to preserve due to the lack of skeleton. The benthic autotrophs are typically difficult to bury due to the strong oxidation at the shallow water, though the decrease in grazing pressure resulting from the faunal mass extinction favors their preservation. Second, in comparison with the faunas, the microbes are difficult to identify on the basis of morphology. Application of advanced analytic techniques is one of the key issues in tracing the microbial records in the Earth history. Recent advancement on this is the proposal of some microbial-induced sedimentary

structures (MISS), some of which were previously suggested to be of inorganic origins. Molecular and isotopic stratigraphy is widely used in the investigation of microbes in the sedimentary rocks with low organic maturity. The fingerprints of microbial lipid biomarkers enable an enhanced molecular investigation on the microorganisms preserved in ancient rocks, favoring the understanding of the biotic crisis on the basis of a comprehensive knowledge related to both the top and the bottom members of the whole marine ecosystem.

Among the various functional groups, cyanobacteria are a kind of photosynthetic bacteria and inhabit widely in the Earth environments. These microorganisms have survived in the Earth for about 2.7 billion years and are believed to be one of the major primary producers in the marine ecosystem. Presence of cyanobacteria during the critical periods in the Earth history could be recorded either by the particular biomarkers, such as the well known 2-methylhopanoids or by the microbialite present during the faunal extinction periods. We reviewed here the recent achievements of the cyanobacterial records to decipher the pattern and causes of the Permo/Triassic faunal mass extinction in marine ecosystems, in particular from the records reported in South China.

2 Cyanobacterial fingerprint for the two-episodic extinction across the PTB

2.1 Cyanobacterial record

To date, we could compile the cyanobacterial record spanning a period of 3 million years at Meishan section in South China where the GSSP is defined (Fig. 1). On the basis of the 2-methyhopane index measured on outcrop samples, Xie et al. (2005) first proposed the occurrence of two episodes of cyanobacterial blooms (bed 26 and bed 29, respectively) coupled with the two horizons of faunal mass extinction (bed 25 and bed 28, respectively) across the PTB at Meishan section. The two cyanobacterial blooms

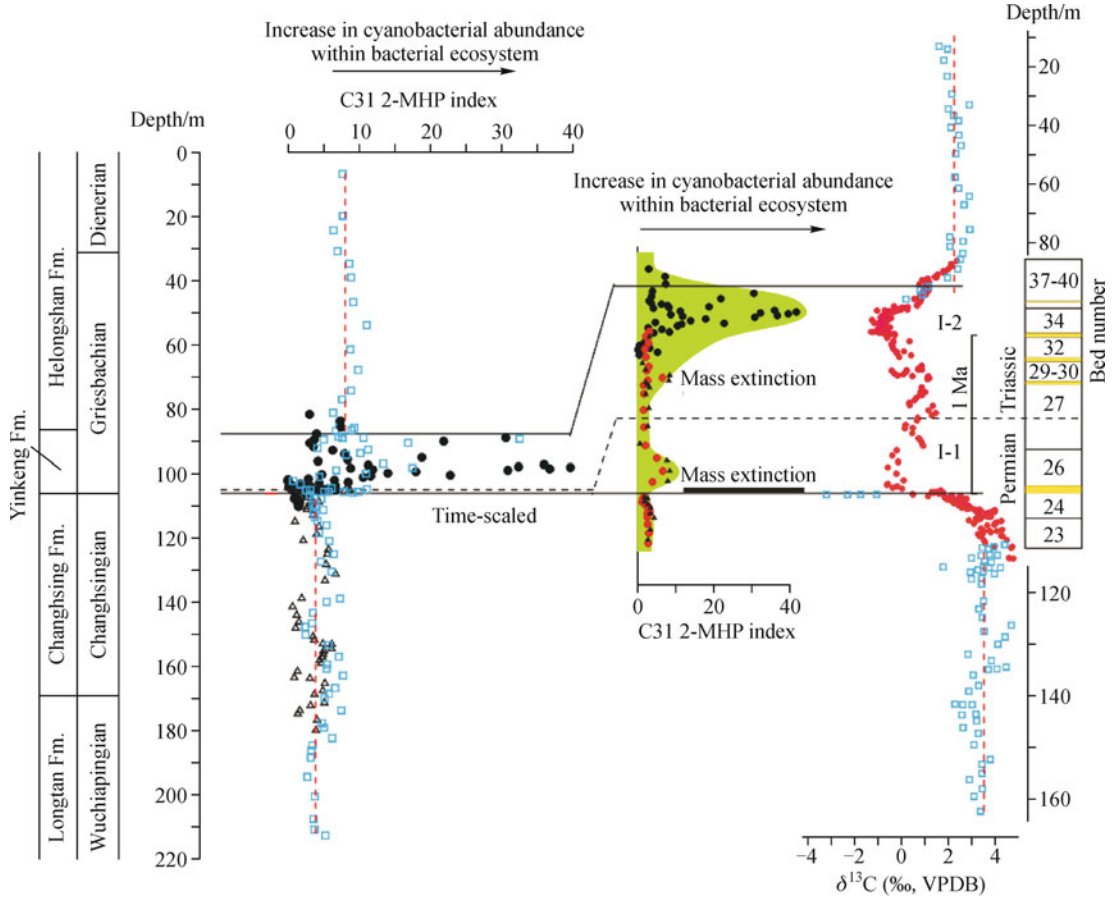

Fig. 1 Compiled trends of the long-term (ca. 3 Ma) variations of cyanobacterial abundance inferred by 2-methylhopane (C31 2-MHP) index, along with the profile of carbon isotope composition (δ^{13}C, VPDB) of carbonate in Meishan section, Zhejiang, China. The data with triangles, blocks, and dots are from Wang and Visscher (2007), Cao et al. (2009) and Xie et al. (2005, 2007), respectively. The red dashed lines show the background values of C31 2-MHP index and δ^{13}Ccarb. The time scale is calculated on the basis of the dating data from Bowring et al. (1998). I-1 and I-2 show the two episodes of the connection among cyanobacterial expansions, shifts in carbon isotope composition, and faunal mass extinction. Redrawn from Xie et al. (2009)

reported were later reproduced by Wang and Visscher (2007) within the same interval at Meishan section. The values of the 2-methylhopane index are comparable between the two studies on the outcrop samples.

Later on, on the basis of the high-resolution molecular investigation in a much large range of strata upward the Meishan section, many maxima in 2-methyhopane index were identified, and the second episode of cyanobacterial blooms (bed 29) following the second pulse of faunal mass extinction at bed 28 was then expanded to bed 37 (Xie et al., 2007, 2009), with maxima of 2-methylhopane index being found up to 41% at bed 34. The expanded and time-scaled second episode (Xie et al., 2007, 2009), composed of several maxima of 2-methyhopane index, was interrupted by several lower values that might result from the local factors. The two episodic blooms of cyanobacteria are found to be associated not only with the two horizons of faunal mass extinction but also with both the negative excursions of carbon isotope composition of carbonate and the enhanced land erosions (Xie et al., 2007). Their close connections are further supportive of the division of the two episodes of cyanobacterial blooms at Meishan, inferring two episodic changes occurred in the Earth surface system. As such, the first episode of cyanobacterial blooms mainly occurs at the *Clarkina* (*Neogondolella*) *meishanensis* and the second one at *Isarcicella isarcica*. This correlation with the conodont zones favors the global comparison of the microbial records.

It is noteworthy that the two episodes reported in the eastern Tethys could be reproduced in the western Tethys. At Bulla section in North Italy, 2-methyhopane index shows two intervals composed of maxima (Fig. 2). The first one occurs at the top of *Neogondolella meishanensi* to the base of *Hindeodus parvus*, and the second one is located at the base of *Isarcicella isarcica*. A slight difference here is that the first episode extends to the conodont zone of *Hindeodus parvus*, spanning a much long strata interval in this shallow water environment in comparison with the deepwater Meishan record. However, the first bloom does extend into the zone of *Hindeodus parvus* at the shallow water in South China, though not at the deep water Meishan section. Microbialites indicative of benthic cyanobacterial blooms after the end-Permian faunal mass extinction were found to occur at *Hindeodus parvus* in several sections in South China, such as Dajiang and Heping in the south-west (Yang et al., 1999; Lehrmann et al., 2003), Huayingshan and Laolongdong in the north (Mu et al., 2009), and Cili and Xiushui in central South China (Wu et al., 2006;Wang et al., 2009). However, it needs to further confirm whether the first cyanobacterial bloom disappears earlier in the deep water sections than in the shallow water sections.

Cao et al. (2009) produced a profile of 2-methylhopane index from core samples at Meishan, comparable with the record of outcrop samples (Xie et al., 2005; 2007; Wang and Visscher 2007), though the former proposed the

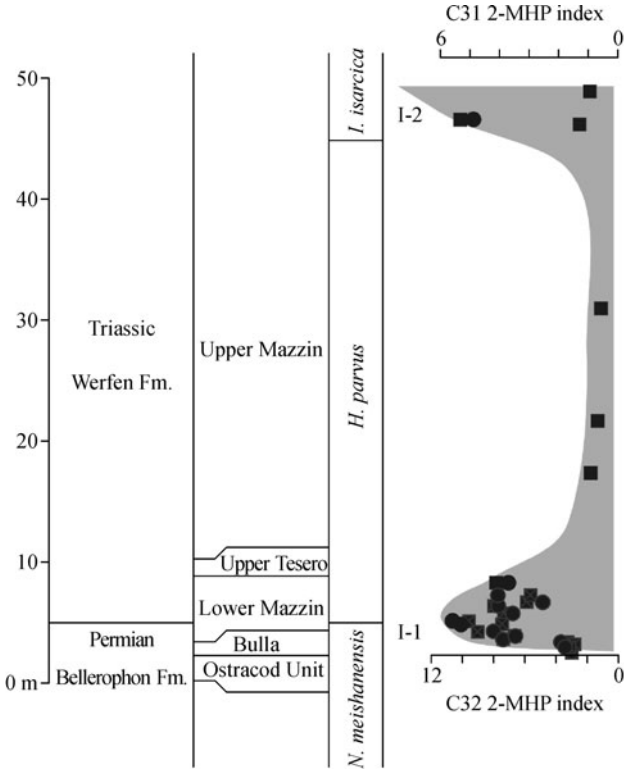

Fig. 2 Variation of cyanobacterial abundance indicated by C31 and C32 2-methyhopane (2-MHP) index (%) in the Bulla section in North Italy, with two spikes being found from the top of *N. meishanensis* to the base of *H. parvus* and at the base of *I. isarcica*. The variation of 2-methylhopane index in the whole *I. isarcica* remains unknown. The solid blocks and dots represent C31 and C32 2-MHP index, respectively. I-1 and I-2 show the two episodes of cyanobacterial expansions. The biostratigraphy is from Farabegoli et al. (2007)

presence of multiple (more than 2) episodes of cyanobacterial blooms. Notably, however, the multiple maxima in 2-methyhopane index in the second episode reported by Xie et al. (2007; 2009) are not contradictory with the multiple episodes of cyanobacterial blooms proposed by Cao et al. (2009); emphasis on the two episodes is not exclusive of the multiple episodes but clearly against monophased record. Both the two and multiple episodes substantially point to the Earth intrinsic factors causing the global biotic crisis and argue against the monophased biotic crisis which is believed to be triggered by the extraterrestrial impact. On this point, the identification of two episodes is necessary to elucidate this intrinsic factor. In fact, if it goes further upward sections and covers the whole Early Triassic, there will be much more episodes of cyanobacterial blooms as shown by the presence of microbialites in the world, which will be further addressed below to show their strong connection with other mass extinctions reported recently in some organism taxa.

Noticeably, the 2-methyhopane index in the second episode shows a maximum much greater than that in the

first episode. This could be caused by the enhanced volcanisms in South China as well as in the world, such as the Siberian flood trap, or the elevated terrestrial erosion resulting from the collapse of terrestrial ecosystems. These geological events will input much more nutrients into the ocean, enabling microbial blooms. In particular, as we discussed later, the Siberian flood trap is tentatively found to postdate the end-Permian mass extinction but could be synchronous with and, thus, responsible for the second episode of global change in the conodont zone of *Isarcicella isarcica*.

Of great significance is the apparent shift of the background values of 2-methyhopane index between the Late Permian and the Early Triassic (Fig. 1). The 2-methyhopane index shows a value generally below 5% in the Late Permian limestones but clearly over 5% in the Early Triassic rocks. This shift would be related to the decrease in grazing pressure in the ocean after the faunal mass extinction, causing the overall expansion of cyanobacteria. On this point, the maxima of 2-methyhopane index during the extinction horizons could be caused by other factors (such as enhanced CO_2 and global warming resulting from volcanisms, anoxia, or enhanced nutrient input, etc.) under the decrease in grazing pressure, and these factors also drive the faunal extinction, negative excursion of carbon isotope composition, and terrestrial erosion, causing their strong connections present as a pattern of two episodes.

2.2 Faunal record

Associated with the two episodic cyanobacteria blooms are the two episodic extinctions of faunas at Meishan section. In particular, faunal mass extinction was proposed to occur as two episodes throughout the whole South China (Fig. 3), although multiple (more than 2) episodic extinctions have been proposed in some sections. The two horizons of biotic crisis were found to be separated by the transitional zone (Yang et al., 1991). In the first episode, trilobites, rugose corals, and fusulinids went extinct; Paleozoic foraminifers, articulate brachiopods, ammonites including the family of Pseudotirolitidae and the genus of *Pseudogastrioceras*, bivalve Aviculopectinidae, gastropods bellerophontids and conodont *Neogondolella* decrease in abundance, and brachiopods lingulids, ammonites including Otoceratidae and Ophiceratidae, bivalve *Emorphotis*, small snails, conodont *Anchignathodus*, and ostracod *Hollinella* increase in abundance (Yang et al., 1991). The second episode is featured by the extinction of Paleozoic foraminifers, ammonites Pseudotirolitidae and *Pseudogastrioceras*, and small snails; the decrease in abundance of brachiopod lingulids, articulate

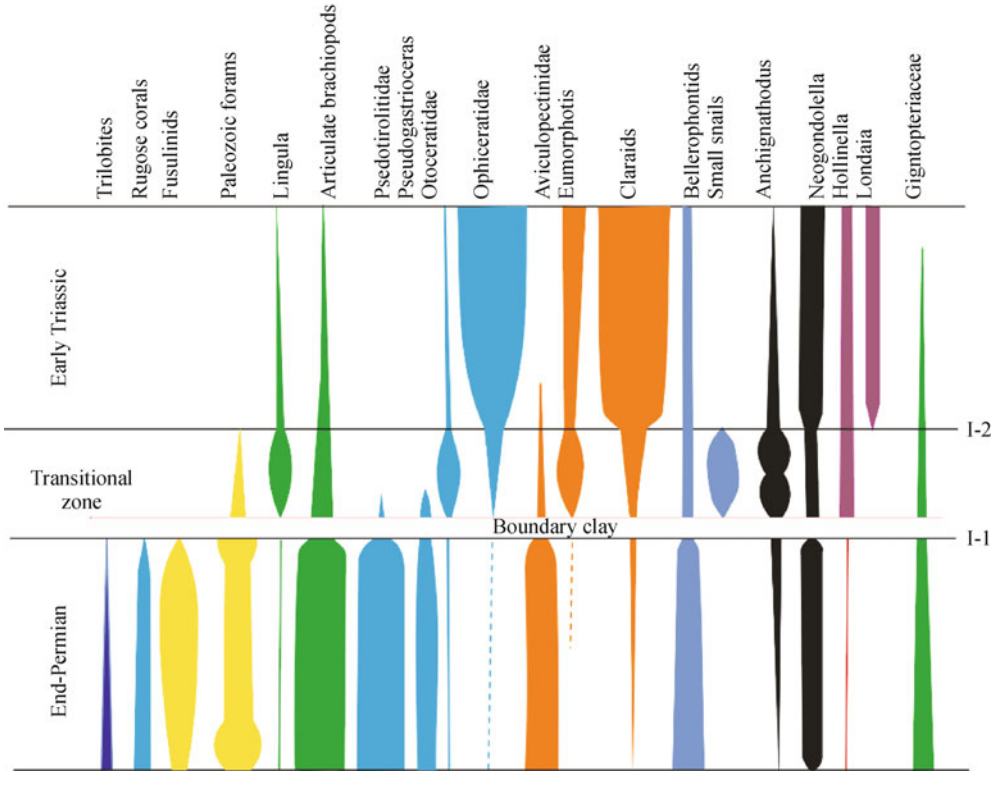

Fig. 3 Compiled data showing the distribution of marine faunas in sections in South China, demonstrating the presence of two episodes of faunal mass extinction separated by a transitional zone (Yang et al., 1991). I-1 and I-2 show the two episodes of faunal mass extinction. The width of the colored columns indicates the relative abundance of faunas

brachiopods, ammonite Otoceratidae, bivalve *Emorphotis*, and conodont *Anchignathodus*; and the increase in abundance of conodont *Neogondolella*, bivalves Claraids, ammonite Ophiceratidae, and ostracod Londaia (Yang et al., 1991). These data from both microbial and faunal records are indicative of the presence of at least two episodes of biotic crisis across the PTB in a wide region.

It is argued that some sections in South China show the presence of monophased faunal mass extinction, rather than two. Mono-phased extinction could be induced by either the Earth intrinsic factors or extraterrestrial impact. In contrast, the two-episodic crisis that occurred within a short time period could only be induced by the Earth intrinsic factors. It then could be concluded that an association of one- with two-phased crisis in a specific region could only infer the Earth intrinsic triggers. On this point, identification of two-episodic crisis at some sections is indicative of intrinsic triggers. Actually, the extraterrestrial impact, though emphasized during the year of 2000 and 2003 (Becker et al., 2001; Basu et al., 2003), is found less supportive, and the Earth intrinsic factors, such as volcanism, are now proposed to be the dominant triggers.

2.3 Carbon isotope record

The variation of carbon isotope compositions in a pattern of two episodes is also documented in a variety of sections. We compared the two episodes in isotope record among Meishan section, GK-1 core in the Carnic Alps in Austria, and Shahreza section in central Iran on the basis of the correlation of conodont biostratigraphy (Xie et al., 2007). Recently, the two minima of δ^{13}C are documented, respectively, at PTB and in the *I. isarcica* zone in a diversity of sections in the world (Korte and Kozur, 2010), including the terrestrial sections (MacLeod et al., 2000; Ward et al., 2005; Korte and Kozur, 2010). These records are indicative of the presence of two episodes of carbon isotope excursions in a wide region. It is notable that many more minima of δ^{13}C could be identified within the two episodes at Meishan section, but the global nature of these minima is unknown.

Comparison among coeval samples of varied carbonate content from different localities led Korte and Kozur (Korte and Kozur, 2010) to suggest that δ^{13}Ccarb should represent seawater signal in Shahreza but reflect diagenetically altered signal in Abadeh. They further extrapolated that low δ^{13}Ccarb values at beds 25–26 at Meishan would be of diagenetic origin. To date, the minima of our δ^{13}Ccarb values reported for beds 25–26 at Meishan section (Xie et al., 2007) are the greatest among all the reported data, and no significant correlation is observed between δ^{13}Ccarb and the carbonate content at the two beds (Fig. 4). This infers that our low δ^{13}Ccarb values in low carbonate beds 25–26 reported before (Xie et al., 2007) are not caused by crystallization from diagenetic fluids or meteoric-water diagenesis.

It is of importance that we find the positive correlation ($R^2 = 0.67$, $n = 102$) of carbonate content with δ^{13}Ccarb but not with δ^{18}O in the interval analyzed (from bed 23 to bed 40 at Meishan) (Fig. 4). Such a relationship could not result from the meteoric-water diagenesis because δ^{18}O will more easily suffer from alteration. Furthermore, δ^{13}Ccarb also shows a large variation, *ca*. 2–3 per mil, within a specific carbonate content. These data indicate that two factors drive the variation of δ^{13}Ccarb at Meishan section.

It is interesting to note that the δ^{13}Ccarb data falling into the three (yellow, blue, and green) regions show no significant relationship with the carbonate content (Fig. 4). In the yellow region with the δ^{13}Ccarb range of $-1‰\sim+1‰$, a specific value of δ^{13}Ccarb corresponds to a very large variation (more than 70%) of carbonate content. This indicates that in the yellow region, the δ^{13}Ccarb values greater than -1 ‰ at an individual bed, with the low carbonate content appear to be of original signal. This further infers that the greater values (> -0.65 ‰) we reported for beds 25–26 (Xie et al., 2007) are of seawater signal, but any values below -1 ‰ reported before by others for bed 25 awaits further confirmation of the original signal. Noticeably, the two episodes of carbon isotope excursion are found to be located in the yellow region but with only 2 per mil shift. The 2 per mil shift in the yellow region is associated with the occurrence of volcanic ash (gray beds in Fig. 4), inferring their causal relationship.

Exclusive of the 2 per mil shift possibly contributed by volcanism, there are 3–4 per mil more shift observed at Meishan section. The positive correlation of δ^{13}Ccarb with carbonate content indicates that the 3–4 per mil shift could be either related to or associated with the variation of lithology. However, limestone and clay beds within bed 34 show no discrimination in δ^{13}Ccarb (Xie et al., 2007), inferring that the positive correlation is a reflection of an association rather than a causal relationship between δ^{13}Ccarb and lithology. This would be the case considering the presence of the 4–5 per mil shift in the limestone sections across PTB in the world. Notably, the 3–4 per mil shift is found to occur from bed 23 to bed 24 (from green to yellow region) or from top of bed 34 to bed 40 (from yellow to blue region); the two intervals are associated with sea level changes and are outside the interval of concentrated volcanic ashes (from bed 25 to bed 34) (Fig. 4). It appears that the 3–4 per mil shift associated with lithology variation could be contributed by the sea level changes at Meishan (Zhang et al., 1996) or even in the world. Sea level drop will lead to an enhanced oxidation of organic matter and an elevated input of terrestrial materials and thus an association of negative shift in isotope record with lithology.

Consequently, both the volcanism and sea-level changes explain the *ca*. 6 per mil shift in δ^{13}Ccarb and, thus, the potential causes of the faunal mass extinction at Meishan section. The gradual drop in δ^{13}Ccarb in the latest Permian (beds 23–24 at Meishan) could be a consequence of sea

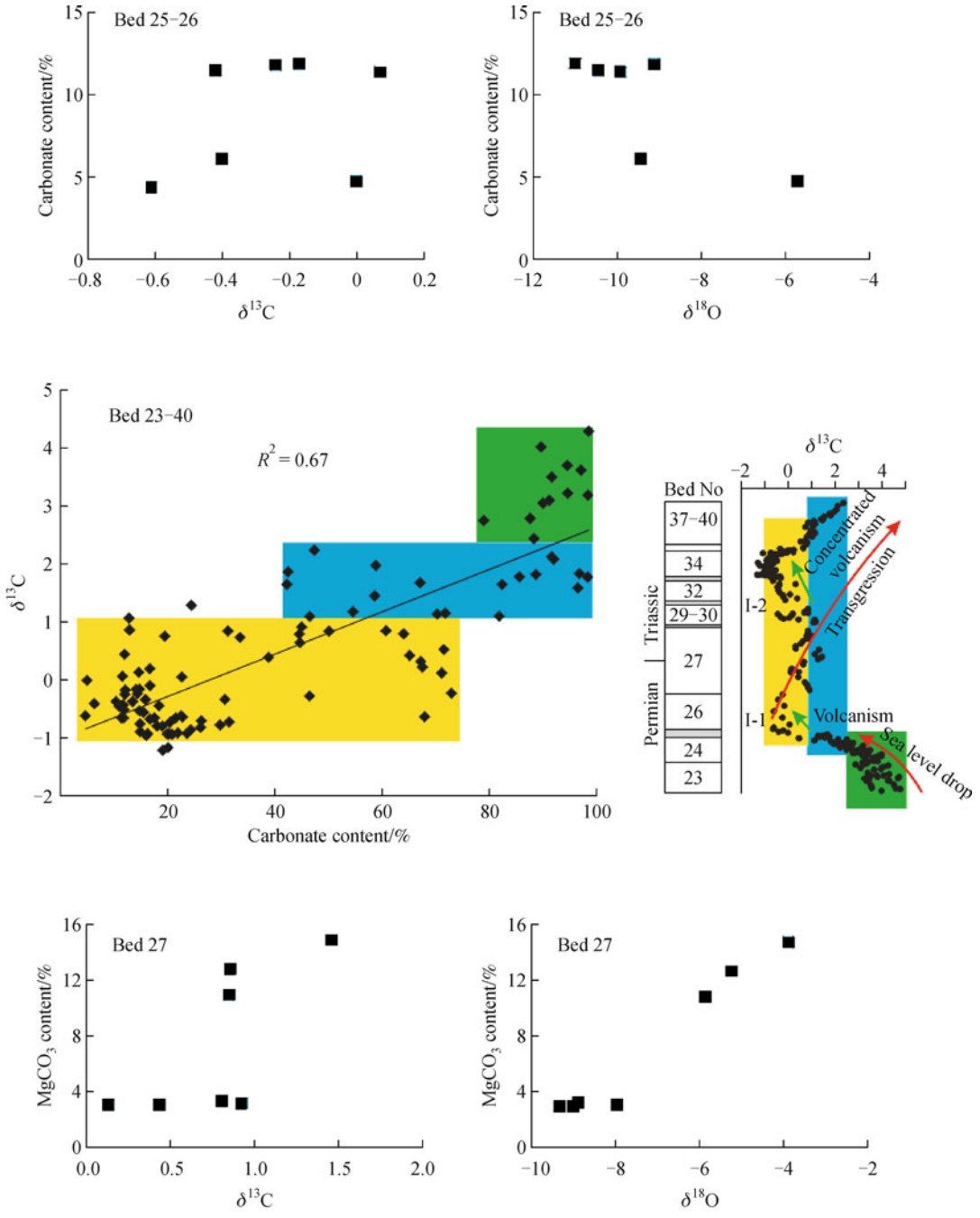

Fig. 4 Plots showing the relationship of δ^{13}C and δ^{18}O with carbonate content for beds 23–40 at Meishan section. The yellow, blue, and green regions show, respectively, the insignificant correlation between δ^{13}C and carbonate content. The gray beds indicate the volcanic ash. Both sea level changes and volcanism are shown to account for the δ^{13}C shift observed at Meishan. I-1 and I-2 show the two global changes

level drop, followed by a further drop of δ^{13}Ccarb (beds 25–26) driven by volcanism (I-1, Fig. 4). The waning of volcanism left a strong signal of transgression on the enhanced δ^{13}Ccarb at bed 27. Concentrated volcanism at the interval of beds 28–35 in South China, and probably the addition of Siberian flood basalt, caused a second drop at δ^{13}Ccarb in *I. isarcica* and overthrew the transgression signal at Meishan (I-2, Fig. 4). Notably, the causal relationship between the two episodic faunal mass extinctions and sea level changes was discussed in detail by Yin et al. (2007).

The local driving factor could be observed at bed 27 at Meishan, in which enhanced δ^{13}Ccarb is associated with elevated content of $MgCO_3$ (Fig. 4), though a significant correlation is absent. The close association with $MgCO_3$ content is particularly apparent in δ^{18}O record at bed 27. It

appears that local factors, such as the $MgCO_3$ content (and the salinity), would lead to the variation of δ^{13}Ccarb within individual beds (such as 1 per mil at bed 27), in particular δ^{18}O. However, the local factors cannot affect the identification of the two episodes of carbon isotope shifts as shown above and documented in a wide region in the world. Instead, caution should be taken while considering any enhanced δ^{18}O values across the PTB.

3 Cyanobacterial inference to the presence of multiple extinctions in the Early Triassic

It is known that cyanobacteria bloomed not only in the two intervals across the Permo/Triassic boundary documented in deepwater Meishan section and shallow-water Bulla section but also in other intervals of the whole Early Triassic. Following the first spike of cyanobacterial blooms, which is present as at least two episodes (I-1, I-2, Fig. 5) after the end-Permian faunal mass extinction, is the presence of three more spikes (II, III, IV, Fig. 5) in Early Triassic (Baud et al., 2007). Calcimicrobial mounds (oolites, stromatolites, and oncoids) in the late Griesbachian to Dienerian appear in the carbonate bank of Nanpanjiang basin in South China (Lehrmann et al., 2003), on the margins of Central and Western Neotethys, and on the Pre-Caucasus margin of Paleotethys. The early Smithian microbial episode (oolitic shoals, stromatolites, and oncoids) is mainly recorded on the carbonate ramps of both north and south Neotethys margins (south Turkey, north and central Iran) and on the carbonate platform of the Arabian margin in Oman (Baud et al., 2007). Spathian microbial reef mounds and small microbial domes (Virgin Limestone Member of the Moenkopi Formation) exposed at the Lost Cabin Springs locality in western American continent (Pruss and Bottjer, 2004, 2005; Pruss et al., 2005). Late Spathian calcimicrobial mounds contain the first reef-dwelling calcareous algae on the Paleotethys complex of north-eastern Iran (Baud et al., 1991). The three spikes of microbialites are composed of cyanobacteria, indicative of presence of the three more spikes of microbial blooms after the first spike across the PTB. The three cyanobacterial blooms are demonstrated to be in association with the three negative excursions of carbonate carbon isotope composition (Knoll et al., 2007).

Significantly, recent compilation of global paleontological data revealed that ammonoids and conodonts suffered conspicuous mass extinctions at the three time interval where carbon isotope excursions were observed in the Early Triassic (Stanley, 2009); ammonoids and conodonts

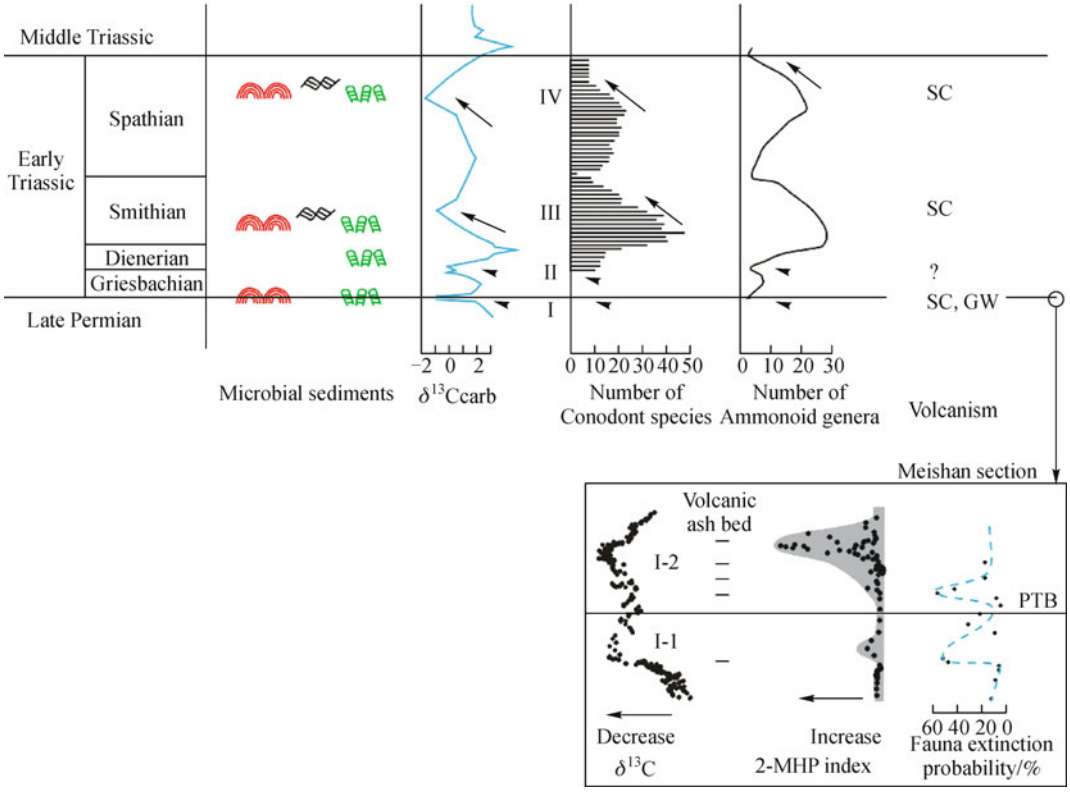

Fig. 5 Compiled curves showing the association among the microbial sediments (indicative of cyanobacterial blooms, Knoll et al., 2007), shifting of carbon cycle (Payne et al., 2004), faunal turnover (Stanley, 2009), and volcanisms in Early Triassic. I, II, III, and IV show the four periods of biotic and environmental events. I-1 and I-2 indicate the two episodic events within the first period. For Meishan section, the faunal extinction probability is calculated on the basis of stratigraphical distribution of species reported by Jin et al. (2000), and the δ^{13}C and 2-MHP are from Xie et al. (2005, 2007). SC-South China, GW-Gondwanaland, and PTB-Permian/Triassic boundary

are believed to be vulnerable to global environmental stress, and the pattern of their diversification and extinction in the Early Triassic turns out to be remarkably similar. In addition to the two taxa, brachiopod communities are also found to go extinct in the Olenekian at Northern Caucasus of Russia (northern Paleo-Tethys), following the short disappearance at PTB (Ruban, 2010); none of the two extinctions of brachiopods is due to the incompleteness of the fossil record, and they are followed by a very rapid radiation in Anisian.

It appears that cyanobacterial blooms are associated with the faunal mass extinction, carbon cycling variations, and land erosion, not only across the PTB, but also in the whole Early Triassic. Episodic cyanobacterial blooms are thus capable of inference to the episodic biotic crisis for 5 million years in the Early Triassic (Fig. 5), and the two episodes across the PTB we reported before (Xie et al., 2005, 2007) are only a part of the series. The protracted recovery previously thought for nearly 5 million years might be thus due to the existence of the multiple extinctions caused by the pulsed environmental stress, and the recovery between extinctions is substantially very rapid. For example, a diverse and complex biota was proposed to recover in shallow, oxygenated environments of the Neo-Tethys oceans in the middle-late Griesbachian age (Twitchett et al., 2004). A rapid recovery of Griesbachian *Meishanorhynchia* association (lower *tulongensis–carinata* zone) from end-Permian mass extinction is documented at the Meishan section, South China, about 1 million years later; the onset of rapid biotic recovery coincided with amelioration of paleoceanographic conditions and an increase in ocean productivity at Meishan (Chen et al., 2007).

Each microbial bloom will naturally stop due to the use up of the resources within a specific habitat, which will cause fluctuated microbial blooms, such as in the I-2 episodes composed of many maxima and minima of 2-methylhopane index. One critical issue is that the four spikes in microbial blooms observed in the Early Triassic arise either solely from the severe end-Permian extinction or from the respective extinctions. On the basis of the strong connection within each spike among microbial blooms, faunal extinctions, and carbon cycling (Fig. 5), we proposed that the episodic blooms resulted from the respective extinctions and the associated environmental stress, rather than solely from the severity of end-Permian mass extinction.

It is notable that the maxima of cyanobacterial blooms are located at the minima of δ^{13}Ccarb in all the four intervals (Fig. 5). However, the two records show an offset with the biotic crisis (Fig. 5). For example, in I-1 episode, cyanobacterial blooms and minima of δ^{13}Ccarb occurred at bed 26, while faunal mass extinction occurred at bed 25. In I-2, faunal mass extinction occurred at bed 28, while cyanobacterial blooms and minima of δ^{13}Ccarb occurred from bed 29 to bed 37. In episodes III and IV, faunal turnover occurred during the progressive transition from minima to maxima of δ^{13}Ccarb, i.e., a lag from the spike of cyanobacterial blooms and minima in δ^{13}Ccarb. That is, the minima of δ^{13}Ccarb postdate the horizon of faunal mass extinction in I-1 and I-2 but predate the biotic crisis at III and IV. Actually, the positive excursions of δ^{13}Ccarb are found to be in association with biotic crisis at I-2 and III. However, the temporal sequence of these geochemical and paleontological events awaits high-resolution investigations on the same section.

4 Cyanobacterial records suggestive of the volcanism as the potential causes of biotic crisis

The extraterrestrial impact, proposed to be one of the possible triggers of the Permo/Triassic biotic crisis during the year of 2000 and 2003 (Becker et al., 2001; Basu et al., 2003), is now found to have less supportive evidence. The Earth intrinsic factors, such as volcanism, sea level changes, paleoclimate change, anoxic condition, and euxinia are becoming the dominant causes proposed. The strong connection among cyanobacterial blooms, faunal mass extinction, and carbon cycling (Fig. 5) suggests that any causes proposed should explain all the comparable trends as we observed throughout the whole Early Triassic. Cyanobacterial records might be indicative of the potential causes of the episodic faunal mass extinction (or the protracted recovery as previously thought).

It is found that cyanobacterial blooms are associated with negative excursions of carbonate carbon isotope composition in the whole Early Triassic. All these intervals are featured by the presence of volcanic rocks in South China, suggesting their causal relationship. At Meishan, the two episodes of cyanobacterial bloom (Xie et al., 2005, 2007) were found in the intervals characterized by the occurrence of altered clay beds of volcanic origin. The 2-methyhopane index exponentially increases in each episode immediately after the volcanic ash (bed 25 and bed 28, respectively) (Fig. 6). Furthermore, the cyanobacterial bloom inferred from the 2-methylhopane index is much greater in the second episode (I-2) than in the first episode (I-1), consistent with the presence of more altered clay (volcanic ashes) beds in I-2. Spatiotemporal relationship between cyanobacterial blooms and volcanic materials was recently identified (Xie et al., 2010). Spatially, the duration of the first cyanobacterial bloom (corresponding to bed 26 at Meishan) is documented to show relationship with the intensity of volcanisms in South China. The initial cyanobacterial bloom has the longest duration and is associated with a prominent Eu anomaly in south-western China, where the most intensive volcanism has been proposed to occur. The duration of microbialites tends to decline northward and eastward, consistent with the waning volcanic influence (Xie et al., 2010). Temporally,

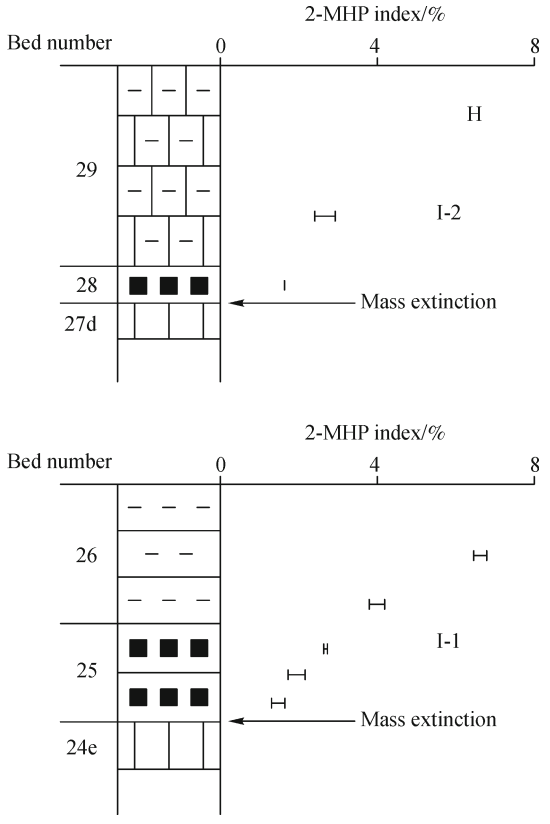

Fig. 6 The 2-methyhopane (2-MHP) index indicative of the two exponential increases in the relative abundance of cyanobacteria immediately after the volcanic ash bed 25 and bed 28 at Meishan (Xie et al., 2005), inferring their causal relationship. It is notable that the maximum of the 2-methylhopane index in core samples could be over 10% for the two episodes (Cao et al., 2009)

cyanobacterial blooms in the whole Early Triassic are associated with known volcanic events in South China and with the largest negative carbon isotope excursions. For example, volcanic ash of Smithian and Spathian age was documented, respectively, in West Pingdingshan (Tong et al., 2003) and in Guangdao (Lehrmann et al., 2006; Galfetti et al., 2007), South China.

It is found that in some microbialite sections in South China, some conodont zones could not be identified, inferring the presence of the erosion or missing of some sediments. However, the deposition absence, if present, could not result in the observed spatial variation of the microbialite in South China.

We proposed that volcanism might be responsible for the microbial blooms in the Early Triassic and their temporal association with carbon isotope excursions and faunal mass extinction (Xie et al., 2010), and here, we expand the discussion further. First, volcanism is an important source of nutrients to the oceans (Weissert and Erba, 2004). It is widely recognized that airborne ash from volcanic eruptions plays important roles on the surface ocean biogeochemical cycle of iron, a key micronutrient for phytoplankton growth (Duggen et al., 2010); the addition of minor amounts of Fe to surface waters can trigger large phytoplankton blooms in the ocean regions with high-nutrient low chlorophyll, which have plenty of macro-nutrients (nitrate and phosphate) but are Fe-limited (Duggen et al., 2010). An iron increase greater than 2nM is experimentally demonstrated to be sufficient to cause a massive phytoplankton bloom (Wells, 2003), and it is calculated that the ash deposition of 1mm over the ocean may raise the surface ocean iron concentrations by a few nM (Duggen et al., 2007). The wide distribution of thick volcanic ash (several centimeters in some locations) in South China across the PTB would stimulate, via enhancing Fe influx, the blooms of chemoautotrophs, including cyanobacteria.

Second, enhanced growth of some cyanobacteria in modern oceans has been demonstrated to physiologically respond to the elevated pCO_2. For example, the cyanobacterium *Trichodesmium*, a predominant diazotroph (nitrogen-fixing) in large parts of the oligotrophic oceans, is demonstrated to physiologically respond with increased carbon and nitrogen fixation at elevated pCO_2 (Czerny et al., 2009). It is found that doubled pCO_2 will enhance the growth of *Microcystis aeruginosa*, a bloom-forming cyanobacterium, by 52%–77% (Qiu and Gao, 2002). The frequent volcanic eruption will release a large amount of CO_2 into the atmosphere, and the enhanced volcanism-induced atmospheric CO_2 levels (Weissert and Erba, 2004) would thus greatly favor cyanobacterial growth.

Third, climatic change is proposed to be a potent catalyst for modern cyanobacterial blooms (Paerl and Huisman, 2008), and cyanobacteria are found to grow better at higher temperatures than other phytoplankton species (Paerl and Huisman, 2008). The enhanced volcanism-induced atmospheric CO_2 levels and other greenhouse gases in the Early Triassic will lead to the global warming (Wignall and Twitchett, 1996) and, thus, blooming of cyanobacteria in the oceans. Global warming could further cause stratification of water column, which in turn results in anoxic condition. Anoxia and even euxinia were widely documented across PTB (Wignall and Twitchett, 1996; Grice et al., 2005), though varied in different locality in both intensity and time duration. Anoxic oceans would remobilize phosphate from the sediments, and thus, a high pCO_2 and phosphorus is favorable for N-fixers to dominate.

Consequently, South China volcanism (or South-east Asian volcanism) around the PTB could have played, via multiple processes, a much larger role in the changes of bacterial ecosystem. It is known that the volcanic eruptions could lead to the negative excursions of carbon isotope compositions via CO_2 input in the Early Triassic. The importance of volcanism-induced CO_2 to the faunal changes is also documented in the Early Triassic, in which the hypercapnia, i.e., physiologic effects of elevated pCO_2, is believed to best account for the selective survival (i.e., the unskeletonized group) of marine invertebrates

(Knoll et al., 2007); calcified organisms, such as corals, foraminifers, green algae, and red algae disappeared, but a great number of their unskeletonized/uncalcified relatives/clades did not. The fact that taxa least sensitive to hypercapnic stress dominated most Early Triassic deposits (Knoll et al., 2007) also suggests the important roles of CO_2 playing in the protracted recovery followed the end-Permian extinction. It is well known that rates of biogenic calcification will greatly decrease in association with pCO_2 rise (Andersson et al., 2005). At these points, volcanism could result in the presence of the close associations for multiple intervals among cyanobacterial blooms, negative excursion of carbon isotope composition and faunal mass extinction.

Association of microbial blooms with faunal extinction results not only from the enhanced volcanism-induced CO_2 level but also from their interactions. It is notable that volcanism causing the faunal mass extinction will further lead to the decrease of grazing pressure. The adverse impact of volcanism on metazoan diversity could have also allowed cyanobacteria to flourish (Xie et al., 2005). On these points, cyanobacterial records are one of the fingerprints of the potential causes of the biotic crisis and the global change at this critical period in the Earth history.

The latest work demonstrated the synchroneity of Emeishan volcanisms with Guadalupian-Lopingian faunal mass extinction in South China (Wignall et al., 2009). It appears that episodic volcanisms, particularly in South China and South-east Asia, could be one of the significant triggers for the biotic crises of at least 9 Ma in Paleozoic, a possible consequence of Pangea formation. It should be pointed out, however, that while the volcanisms in South China and South-east Asia are emphasized, volcanism activities elsewhere around the Permo/Triassic boundary could also contribute a lot to the global changes; volcanism activities were widespread along the western Panthalassa margin, in Primorye (Vrzhosek, 1997) and Gondwanaland (Veevers and Tewari, 1995), which may be linked with convergent plate tectonics or rifting, and it should have been subducted at what is now the Pacific margin (Yin et al., 2007). However, we proposed that Siberian flood trap could be responsible for the Early Triassic extinctions (or the protracted recovery as previously thought), but its synchronicity with the end-Permian extinction await more precise dating data to confirm.

5 Major Siberian eruptions and the end-Permian faunal mass extinction

It is previously accepted that the well-known Siberian flood basalt is synchronous with and, thus, responsible for the end-Permian mass extinction. However, on the basis of the new dating data from both U/Pb zircon and $^{40}Ar/^{39}Ar$ methods, we proposed that major Siberian basalt eruption postdates the end-Permian mass extinction. Due to space limitation, we did not go any further to make a full explanation on the dating correlation before (Xie et al., 2010), and thus, a more detailed discussion is presented herein (Fig. 7).

First of all, the transition from Permian to Triassic fossil assemblage was suggested to begin well before the basalt eruption (Sadovnikov, 2008) in Nidymsky suite in Lower Tunguska River. This provides the strong biostratigraphi-

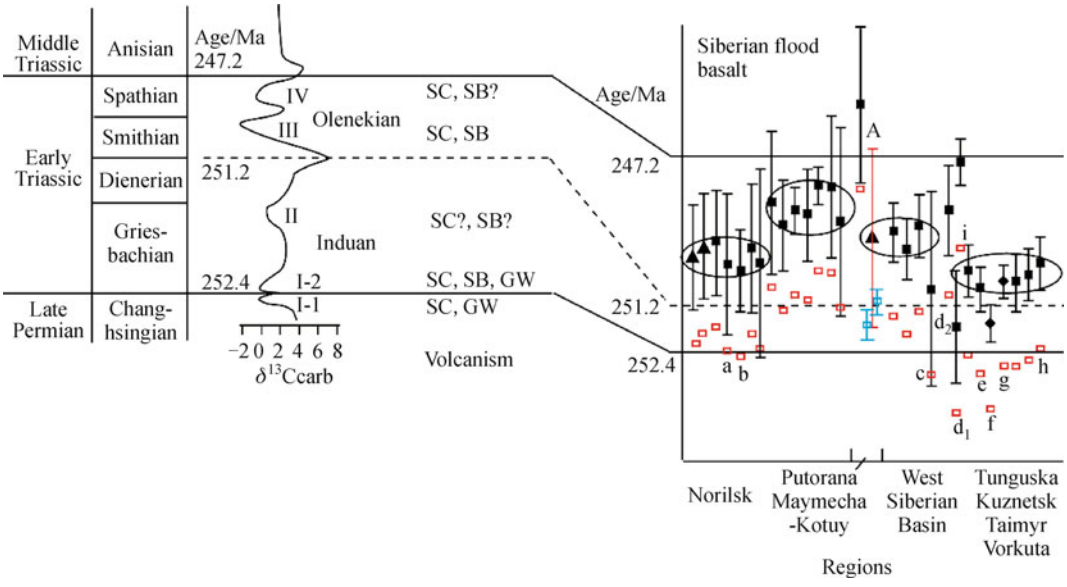

Fig. 7 Profile of $\delta^{13}C$ in Early Triassic (Payne et al., 2004) and the dating data of Siberian flood basalt (Saunders and Reichow, 2009). The red blocks are corrected to U/Pb dating data from the $^{40}Ar/^{39}Ar$, and the blue data are the U/Pb dating values measured. The boundaries are indicated by U/Pb dating data from Lehrmann et al. (2006), Galfetti et al. (2007) and Mundil et al. (2004). I-1, I-2, II, III, and IV show the shifts in carbon isotope composition. SC-South China, SB-Siberian, GW-Gondwanaland

cal evidence of the volcanism postdating.

Second, new U/Pb dating on individual zircon grains from the ash beds at Meishan sections changed the end-Permian mass extinction age from 251.4±0.7 Ma (Bowring et al., 1998) to 252.4±0.3 Ma (Mundil et al., 2004), raising nearly 1 Ma difference. The only available U/Pb dating data of Siberian basalt ranging from 251.7±0.4 to 251.3±0.3 Ma were previously proposed to be synchronous with the old age (251.4±0.7 Ma) of the end-Permian mass extinction (Kamo et al., 2003), but it clearly should postdate the new age (252.4±0.3 Ma) of end-Permian biotic crisis. The U/Pb dating of individual zircon grains from both Meishan ash and Sibeiran basalt provides the second line of evidence for the volcanism postdating.

Third, the compiled $^{40}Ar/^{39}Ar$ dating data of Siberian basalt are proposed to be comparable with the $^{40}Ar/^{39}Ar$ dating data of ash beds at Meishan section and thus be synchronous with the end-Permian mass extinction (Reichow et al., 2009; Saunders and Reichow, 2009). However, the error bars of $^{40}Ar/^{39}Ar$ dating are too large to be precisely correlated between the biotic and the volcanic events. It is notable that the $^{40}Ar/^{39}Ar$ dating value (Fig. 7, A) of Maymecha basalt in the Siberian region associated with the only known U/Pb dating data clearly encloses most of the $^{40}Ar/^{39}Ar$ dating data of Siberian basalt (with only 4 samples outside this range). Based on this, considering their error bars, these $^{40}Ar/^{39}Ar$ dating data of Siberian basalt enclosed by this U/Pb constrained $^{40}Ar/^{39}Ar$ dating should also postdate the end-Permian mass extinction.

Fourth, it is well-known that the difference is present between U/Pb and $^{40}Ar/^{39}Ar$ dating. There is 1% difference generally used for the correction between them. However, a 1.29% difference is observed between the two dating methods for bed 28 ash in Meishan section, and less than 1% is present for the Siberian basalt. Any correction made for the two dating methods is thus questionable. That is why we did not correct all the $^{40}Ar/^{39}Ar$ dating data; instead, we used the U/Pb dating of Siberian basalt to compare with the PTB U/Pb dating data in Fig. 2 of our previous paper (Xie et al., 2010). We also showed the U/Pb constrained $^{40}Ar/^{39}Ar$ dating to compare with other $^{40}Ar/^{39}Ar$ dating data of Siberian basalt in that figure (Xie et al., 2010), but we did not mean to compare it with the U/Pb dating of the boundary ages.

Generally, however, we here could also correct the mean values of all the $^{40}Ar/^{39}Ar$ dating data of Siberian basalt on the basis of the difference between $^{40}Ar/^{39}Ar$ and U/Pb dating measured on Maymecha basalt in Siberian region (Fig. 7) (a correction of 1% difference would get the similar result). It is clear that most samples from Siberian basalt are located at the horizons over the PTB.

However, some samples are indeed located below the PTB, but it is noticeable that most samples corrected to predate the PTB are from the margin of the Siberian flood trap where lots of intrusive rocks developed. Specifically, samples e, f, and g, much older than the PTB, are clearly not the eruptive rocks but the intrusive rocks (Gabbros) (Reichow et al., 2009).

Sample h corrected to be of the PTB age was taken from the horizon 3.5 m above sample i in Vorkuta, and it is surprising to note that the two samples, with a thickness interval of 3.5 m among the thousands-of-meters thick Siberian basalt, have an age difference of 2.3 Ma.

Sample c from West Siberian basin corrected to predate the PTB shows a very large error, but the three other samples with small errors from the same locality clearly postdate the PTB.

Samples d1 and d2 are both from Nidymsky suite in Lower Tunguska River but have an age difference of 3Ma. Just in this area, however, the transition from Permian to Triassic fossil assemblage was suggested to begin well before the basalt eruption (Sadovnikov, 2008).

Samples a and b corrected to be at the PTB were taken from the top of the Norilsk basalt, and they are surprisingly older than the samples from the bottom of Norilsk basalt.

Consequently, even corrected by the U/Pb dating, few samples are substantially located at the PTB after the exclusion of the questionable data (samples a, b, c, d1, e, f, g, and h), i.e., most $^{40}Ar/^{39}Ar$ dating data of Siberian flood trap are relatively younger than the PTB age, which means the major eruptions postdated the end-Permian mass extinction.

To sum up, either on the basis of biostratigraphical data (Sadovnikov, 2008), the U/Pb dating of individual zircon grains (Xie et al., 2010) or the U/Pb corrected $^{40}Ar/^{39}Ar$ dating shown here, the major eruptions of the Siberian basalt postdate the end-Permian mass extinction. It is possible, however, that the Siberian flood basalt might contribute to the second episode of faunal mass extinction corresponding to bed 28 at Meishan, and the other extinctions in the Early Triassic. The 2-methylhopane index in the second episode is much greater than that in the first episode at Meishan section, which would be a part of consequence of this volcanism addition. The final confirmation of their synchroneity, however, awaits much more precise U/Pb dating in the future. Particularly, it is notable that cautions should be taken in the confirmation of the dating data; we need to make sure that dating is conducted on eruptive rocks rather than intrusive rocks.

6 Future work

Microbial records in South China suggest the important contribution of volcanism that occurred in this region and surroundings to the biotic crisis. However, the spatial and temporal distribution of these volcanisms remains largely unknown due to the lack of the high-resolution record of volcanic ash. It is of great significance to investigate the occurrence of volcanic materials in the South-eastern Asia, which in turn helps to decipher the volcanism intensity and

the origin of volcanic materials. Furthermore, volcanism that occurred in other regions, such as those around the Gondwanaland and Panthalassa margin, is to be investigated so that a time framework of volcanisms could be reconstructed. The Siberian flood basalt in particular awaits more precise U/Pb dating to confirm or veto its contribution to the end-Permian mass extinction. Only when these are done can we reconstruct the temporal variation of volcanism resulting from Pangea formation and thus substantially understand the causal relationship among the volcanism, faunal mass extinction, microbial changes, and carbon cycle perturbation.

More evidence is now accumulating to infer a long-term biotic crisis driven by the intrinsic factors (such as volcanism and sea level change) across the PTB. Environmental and biotic effects, if driven by these intrinsic triggers, will vary in intensity, amplitude, and time sequence, depending on the geographical locations or geological conditions. This will result in a consequence of paleogeographical variation in these events that are different from those induced by the extraterrestrial impact. The observed spatiotemporal variations in the distribution of both microbialite and volcanic materials in South China (Xie et al., 2010) are such kind of reflection. Some investigations have shown that the biotic crisis starts early in the deep ocean within the marine ecosystem, while some evidence supports the initial collapse of terrestrial ecosystem ahead of marine ecosystem. They both point to a trigger originating from the Earth interior. Difference in spatial variation of the environmental and biotic events could be one of the key issues to be investigated in the future to strengthen the Earth intrinsic triggers.

The long-term perturbation of carbon cycle is suggestive of the feedback of the Earth system to the forces played on it, via partly the interaction between environments and organisms. However, less work is conducted concerning the active biotic roles, though some biotic responses to the harsh environmental condition are known. In particular, the wide distribution of microbial sediments in the Early Triassic could, to some extent, alter the deteriorated environments via the carbon cycle. Microbial roles on the shift of past environments await further investigation, making it possible to morph paleontology into geobiology in the future.

7 Conclusions

Microbes are documented to be in sensitive responses to both the pattern and causes of the 5-million-year biotic crisis from the latest Permian to the end of the Early Triassic. Two episodic cyanobacterial blooms were observed to couple with carbon isotope excursions and faunal mass extinction at Meishan section, suggestive of the presence of at least two global changes across the PTB. Close associations among the three records (cyanobacterial bloom, shift in carbon isotope composition, and faunal extinction) were subsequently observed in three intervals in the Early Triassic. Cyanobacterial record is thus suggestive of the presence of multiple episodes of biotic crises lasting from end-Permian to the end of the Early Triassic. Spatiotemporal association of cyanobacterial blooms with volcanic materials in South China, and probably in South-east Asia, infers their causal relationship. The volcanism, in association with sea-level change, is believed to trigger the biotic crisis in several ways and to cause the close association among microbial blooms, the carbon isotope excursions, and faunal mass extinctions in four intervals in the Early Triassic. Difference in spatial variation of the environmental and biotic events could be one of the key issues to be investigated in the future to strengthen the Earth intrinsic triggers.

Acknowledgements This work was supported by the National Basic Research Program of China (No. 2011CB808800), the National Natural Science Foundation of China (Grant Nos. 40730209, 40921062), and the 111 project (B08030). Special thanks go to Professors E. Farabegoli and M. C. Perri for the assistance of sampling in Bulla section.

References

Andersson A J, Mackenzie F T, Lerman A (2005). Coastal ocean and carbonate systems in the high CO_2 world of the anthropocene. Am J Sci, 305(9): 875–918

Basu A R, Petaev M I, Poreda R J, Jacobsen S B, Becker L (2003). Chondritic meteorite fragments associated with the Permian-Triassic boundary in Antarctica. Science, 302(5649): 1388–1392

Baud A, Brandner R, Donofrio D A (1991). The Sefid Kuh limestone—A late Lower Triassic Carbonate Ramp (Aghdarband, Northeast-Iran). Abhandlungen der Geologisches Bundesanstalt in Wien, 38: 111–123

Baud A, Richoz S, Pruss S (2007). The lower Triassic anachronistic carbonate facies in space and time. Global Planet Change, 55(1–3): 81–89

Becker L, Poreda R J, Hunt A G, Bunch T E, Rampino M (2001). Impact event at the Permian-Triassic boundary: evidence from extraterrestrial noble gases in fullerenes. Science, 291(5508): 1530–1533

Bowring S A, Erwin D H, Davidek K, Wang W, Davidek K, Wang W, Jin M W, Martin YG (1998). U/Pb zircon geochronology and tempo of the end-permian mass extinction. Science, 280(5366): 1039–1045

Cao C, Love G D, Hays L E, Wang W, Shen S, Summons R E (2009). Biogeochemical evidence for euxinic oceans and ecological disturbance presaging the end-Permian mass extinction event. Earth Planet Sci Lett, 281(3–4): 188–201

Chen Z, Tong J, Kaiho K, Kawahata H (2007). Onset of biotic and environmental recovery from the end-Permian mass extinction within 1–2 million years: A case study of the Lower Triassic of the Meishan section, South China. Palaeogeogr Palaeoclimatol Palaeoecol, 252 (1–2): 176–187

Czerny J, Barcelos e Ramos J, Riebesell U (2009). Influence of elevated CO_2 concentrations on cell division and nitrogen fixation rates in the bloom-forming cyanobacterium *Nodularia spumigena*. Biogeos-

ciences, 6(9): 1865–1875

Duggen S, Croot P, Schacht U, Hoffmann L (2007). Subduction zone volcanic ash can fertilize the surface ocean and stimulate phytoplankton growth: Evidence from biogeochemical experiments and satellite data. Geophys Res Lett, 34(1): L01612

Duggen S, Olgun N, Croot P, Hoffmann L, Dietze H, Delmelle P, Teschner C (2010). The role of airborne volcanic ash for the surface ocean biogeochemical iron-cycle: a review. Biogeosciences, 7(3): 827–844

Farabegoli E, Perri M C, Posenato R (2007). Environmental and biotic changes across the Permian-Triassic boundary in western Tethys: The Bulla parastratotype, Italy. Global and Plametary Change, 55: 109–135

Galfetti T, Bucher H, Ovtcharova M, Schaltegger U, Brayard A, Brühwiler T, Goudemand N, Weissert H, Hochuli P A, Cordey F, Kuang G D (2007). Timing of the Early Triassic carbon cycle perturbations inferred from new U/Pb ages and ammonoid biochronozones. Earth Planet Sci Lett, 258(3–4): 593–604

Grice K, Cao C, Love G D, Böttcher M E, Twitchett R J, Grosjean E, Summons R E, Turgeon S C, Dunning W, Jin Y (2005). Photic zone euxinia during the Permian-triassic superanoxic event. Science, 307 (5710): 706–709

Jin Y G, Wang Y, Wang W, Shang Q H, Cao C Q, Erwin D H (2000). Pattern of marine mass extinction near the Permian-Triassic boundary in South China. Science, 289(5478): 432–436

Kamo S L, Czamanske G K, Amelin Y, Fedorenko V A, Davis D W, Trofimov V R (2003). Rapid eruption of Siberian flood-volcanic rocks and evidence for coincidence with the Permian-Triassic boundary and mass extinction at 251 Ma. Earth Planet Sci Lett, 214(1–2): 75–91

Knoll A H, Bambach R K, Payne J L, Pruss S, Fischer W W (2007). Paleophysiology and end-Permian mass extinction. Earth Planet Sci Lett, 256(3–4): 295–313

Korte C, Kozur H W (2010). Carbon-isotope stratigraphy across the Permian–Triassic boundary: A review. J Asian Earth Sci, 39(4): 215–235

Lehrmann D J, Payne J L, Felix S V, Dillett P M, Wang H, Yu Y Y, Wei J Y (2003). Permian–Triassic boundary sections from shallow-marine carbonate platforms of the Nanpanjiang Basin, south China: implications for oceanic conditions associated with the end-Permian extinction and its aftermath. Palaios, 18(2): 138–152

Lehrmann D J, Ramezani J, Bowring S, Martin M W, Montgomery P, Enos P, Payne J L, Orchard M J, Wang H M, Wei J Y (2006). Timing of recovery from the end-Permian extinction: Geochronologic and biostratigraphic constraints from south China. Geology, 34(12): 1053–1056

MacLeod K G, Smith R M H, Koch P L, Ward P D (2000). Timing of mammal-like reptile extinctions across the Permian–Triassic boundary in South Africa. Geology, 28(3): 227–230

Mu X, Kershaw S, Li Y, Guo L, Qi Y, Reynolds A (2009). High-resolution carbon isotope changes in the Permian-Triassic boundary interval, Chongqing, South China; implications for control and growth of earliest Triassic microbialites. J Asian Earth Sci, 36(6): 434–441

Mundil R, Ludwig K R, Metcalfe I, Renne P R (2004). Age and timing of the Permian mass extinctions: U/Pb dating of closed-system zircons. Science, 305(5691): 1760–1763

Paerl H W, Huisman J (2008). Climate. Blooms like it hot. Science, 320 (5872): 57–58

Payne J L, Lehrmann D J, Wei J, Orchard M J, Schrag D P, Knoll A H (2004). Large perturbations of the carbon cycle during recovery from the end-permian extinction. Science, 305(5683): 506–509

Pruss S B, Bottjer D J (2004). Late Early Triassic microbial reefs of the Western United States: a description and model for their deposition in the aftermath of the end-Permian mass extinction. Palaeogeogr Palaeoclimatol Palaeoecol, 211(1–2): 127–137

Pruss S B, Bottjer D J (2005). The reorganization of reef communities following the end-Permian mass extinction. C R Palevol, 4(6–7): 553–568

Pruss S B, Corsetti F A, Bottjer D J (2005). The unusual sedimentary rock record of the Early Triassic: a case study from the southwestern United States. Palaeogeogr Palaeoclimatol Palaeoecol, 222(1–2): 33–52

Qiu B, Gao K (2002). Effects of CO_2 enrichment on the bloom-forming cyanobacterium *Microcystis aeruginosa* (cyanophyceae): Physiological responses and relationships with the availability of dissolved inorganic carbon. J Phycol, 38(4): 721–729

Reichow M K, Pringle M S, Al'Mukhamedov A I, Allen M B, Andreichev V L, Buslov M M, Davies C E, Fedoseev G S, Fitton J G, Inger S, Medvedev A Y, Mitchell C, Puchkov V N, Safonova I Y, Scott R A, Saunders A D (2009). The timing and extent of the eruption of the Siberian Traps large igneous province: Implications for the end-Permian environmental crisis. Earth Planet Sci Lett, 277 (1–2): 9–20

Ruban D A (2010). The Permian/Triassic mass extinction among brachiopods in the Northern Caucasus (northern Palaeo-Tethys): A tentative assessment. Geobios, 43(3): 355–363

Sadovnikov G N (2008). On the global stratotype section and point of the Triassic base. Stratigr Geol Correl, 16: 31–46

Saunders A, Reichow M (2009). The Siberian traps and the End-Permian mass extinction: a critical review. Chin Sci Bull, 54(1): 20–37

Stanley S M (2009). Evidence from ammonoids and conodonts for multiple Early Triassic mass extinctions. Proc Natl Acad Sci USA, 106(36): 15264–15267

Tong J, Zakharov Y D, Orchard M J, Yin H, Hansen H J (2003). A candidate of the Induan-Olenekian boundary stratotype in the Tethyan region. Science in China (Series D), 46: 1182–1200

Twitchett R J, Krystyn L, Baud A, Wheeley J R, Richoz S (2004). Rapid marine recovery after the end-Permian mass-extinction event in the absence of marine anoxia. Geology, 32(9): 805–808

Veevers J J, Tewari R C (1995). Permian–Carboniferous and Permian–Triassic magmatism in the rift zone bordering the Tethyan margin of southern Pangea. Geology, 23(5): 467–470

Vrzhosek A A (1997). Late Permian bimodal volcanism in South Primorye. In: Dickins J M, Yang Z Y, Yin H F, Lucas S G, Acharya S K, eds. Late Palaeozoic And Early Mesozoic Circum-Pacific Events And Their Global Correlation. Cambriage: Cambridge University Press, 106–108

Wang C, Visscher H (2007). Abundance anomalies of aromatic biomarkers in the Permiannt–Triassic boundary section at Meishan, China–Eevidence of end-Permian terrestrial ecosystem collapse. Palaeogeogr Palaeoclimatol Palaeoecol, 252(1–2): 291–303

Wang Q, Tong J N, Song H, Yang H (2009). Ecological evolution across the Permian/Triassic boundary at the Kangjiaping Section in Cili County, Hunan Province, China. Science in China (Series D), 52: 797–806

Ward P D, Botha J, Buick R, De Kock M O, Erwin D H, Garrison G H, Kirschvink J L, Smith R (2005). Abrupt and gradual extinction among Late Permian land vertebrates in the Karoo basin, South Africa. Science, 307(5710): 709–714

Weissert H, Erba E (2004). Volcanism, CO_2 and palaeoclimate: A Late Jurassic–Early Cretaceous carbon and oxygen isotope record. Geological Society of London Journal, 161(4): 695–702

Wells M L (2003). The level of iron enrichment required to initiate diatom blooms in HNLC waters. Mar Chem, 82(1–2): 101–114

Wignall P B, Sun Y, Bond D P G, Izon G, Newton R J, Védrine S, Widdowson M, Ali J R, Lai X, Jiang H, Cope H, Bottrell S H (2009). Volcanism, mass extinction, and carbon isotope fluctuations in the Middle Permian of China. Science, 324(5931): 1179–1182

Wignall P B, Twitchett R J (1996). Oceanic anoxia and the end Permian mass extinction. Science, 272(5265): 1155–1158

Wu Y, Yang W, Jiang H, Fan J (2006). Petrological evidence for the sea level fall across the Permian-Triassic boundary at Xiushui, Jiangxi. Sinica Petrology, 22: 3039–3046

Xie S, Pancost R D, Huang J H, Wignall P B, Yu J, Tang X, Chen L, Huang X, Lai X (2007). Changes in the global carbon cycle occurred as two episodes during the Permian–Triassic crisis. Geology, 35(12): 1083–1086

Xie S, Pancost R D, Wang Y, Yang H, Wignall P B, Luo G, Jia C, Chen L (2010). Cyanobacterial blooms tied to volcanism during the 5 m.y. Permo-Triassic biotic crisis. Geology, 38(5): 447–450

Xie S, Pancost R D, Yin H, Wang H, Evershed R P (2005). Two episodes of microbial change coupled with Permo/Triassic faunal mass extinction. Nature, 434(7032): 494–497

Xie S, Yin H, Cao C, Wang C, Lai X (2009). Episodic changes of the Earth surface system across the Permian-Triassic boundary: molecular geobiological records. Acta Palaeontologica Sin, 48(3): 202–211 (in Chinese)

Yang S, Hao W, Wang X (1999). Conodont Evolutionary Lineages, Zonation and P-T Boundary at P-T Boundary Beds in Guangxi. Beijing: China.Peking University Press, 81–95 (in Chinese)

Yang Z Y, Wu S B, Yin H F, Xu G R, Zhang K X, Bi X M (1991). Permo-Triassic Events of South China. Beijing: Geological Publishing House (in Chinese)

Yin H, Feng Q, Lai X, Baud A, Tong J (2007). The protracted Permo-Triassic crisis and multi-episode extinction around the Permian-Triassic boundary. Global Planet Change, 55(1–3): 1–20

Zhang K, Tong J, Yin H, Wu S (1996). Sequence stratigraphy of the Permian-Triassic boundary section of Changxing, Zhejiang. Acta Geol Sin, 70(3): 270–281